

SU(3) Einstein-Yang-Mills Sphalerons and Black Holes

Burkhard Kleihaus¹, Jutta Kunz^{1,2} and Abha Sood¹

¹Fachbereich Physik, Universität Oldenburg, Postfach 2503
D-26111 Oldenburg, Germany

² Instituut voor Theoretische Fysica, Rijksuniversiteit te Utrecht
NL-3508 TA Utrecht, The Netherlands

May 9, 2018

Abstract

In the SU(3) Einstein-Yang-Mills system sequences of static spherically symmetric regular solutions and black hole solutions exist for both the SU(2) and the SO(3) embedding. We construct the lowest regular solutions of the SO(3) embedding, missed previously, and the corresponding black holes. The SO(3) solutions are classified according to their boundary conditions and the number of nodes of the matter functions. Both, the regular and the black hole solutions are unstable.

Utrecht-Preprint THU-95/8

1 Introduction

The $SU(2)$ Einstein-Yang-Mills system possesses a sequence of static spherically symmetric regular particle-like solutions [1], which are unstable [2, 3]. The n -th solution of the sequence has n nodes and $2n$ unstable modes [4, 5]. The lowest solution has been interpreted in analogy to the electroweak sphaleron [6] as the top of a barrier between vacua [3].

Beside the regular solutions the $SU(2)$ Einstein-Yang-Mills system possesses static spherically symmetric black hole solutions. There are in fact two different types of black hole solutions having the same mass. These are the Schwarzschild black holes with vanishing gauge fields and the $SU(2)$ coloured black holes [7, 8, 9]. Like the regular solutions the coloured black hole solutions are unstable [10, 11, 5]. Thus for a certain range of masses the system possesses two distinct types of black holes, providing a counterexample to the “no-hair conjecture” for black holes, unless the coloured black holes are discarded as a counterexample because of their instability.

Here we consider static spherically symmetric regular solutions and black holes of the $SU(3)$ Einstein-Yang-Mills system (with vanishing time component of the gauge field). Such solutions are obtained for both, the $SU(2)$ embedding and the $SO(3)$ embedding. The $SU(2)$ embedding reproduces the known $SU(2)$ solutions, while the $SO(3)$ embedding leads to new interesting solutions. Missing the lowest regular solutions, several regular $SO(3)$ solutions have been found previously by Künzle [12], but he did not succeed in obtaining the corresponding black holes.

We here construct the first few solutions of a new class of regular $SO(3)$ solutions. These solutions include the lowest regular $SO(3)$ solution, which we have obtained first as a limiting solution of the $SU(3)$ Einstein-Skyrme system [13] (in analogy to the $SU(2)$ case [14]). We classify the $SO(3)$ solutions according to their boundary conditions and the number of nodes of the matter functions.

Analogous to the $SU(2)$ Einstein-Yang-Mills system asymptotically flat $SO(3)$ black hole solutions emerge from the regular solutions by requiring regularity at a finite event horizon. We construct the black hole solutions corresponding to the first few solutions with the least nodes.

The stability of regular and black hole solutions of arbitrary gauge groups has been studied recently [15]. We apply the theorems of Ref. [15] to demonstrate the instability of both regular and black hole $SO(3)$ solutions.

2 $SU(3)$ Einstein-Yang-Mills Equations of Motion

We consider the $SU(3)$ Einstein-Yang-Mills action

$$S = S_G + S_M = \int L_G \sqrt{-g} d^4x + \int L_M \sqrt{-g} d^4x \quad (1)$$

with

$$L_G = \frac{1}{16\pi G}R , \quad (2)$$

and the matter Lagrangian

$$L_M = -\frac{1}{2}\text{Tr}(F_{\mu\nu}F^{\mu\nu}) , \quad (3)$$

where

$$F_{\mu\nu} = \partial_\mu A_\nu - \partial_\nu A_\mu - ie[A_\mu, A_\nu] , \quad (4)$$

$$A_\mu = \frac{1}{2}\lambda^a A_\mu^a , \quad (5)$$

and e is the coupling constant. Variation of the action eq. (1) with respect to the metric $g_{\mu\nu}$ and the gauge field A_μ leads to the Einstein equations and the matter field equations.

To construct static spherically symmetric regular solutions and black holes we employ Schwarzschild-like coordinates and adopt the spherically symmetric metric

$$ds^2 = g_{\mu\nu}dx^\mu dx^\nu = -A^2Ndt^2 + N^{-1}dr^2 + r^2(d\theta^2 + \sin^2\theta d\phi^2) , \quad (6)$$

with

$$N = 1 - \frac{2m}{r} . \quad (7)$$

Generalized spherical symmetry for the gauge field is realized by embedding the SU(2) or the SO(3) generators T_i in SU(3). In the SU(2)-embedding $\vec{T} = \frac{1}{2}(\lambda_1, \lambda_2, \lambda_3)$, and the ansatz for the gauge field has vanishing time component [1],

$$\begin{aligned} A_0 &= 0 , \\ A_i &= \frac{1-w(r)}{2re}(\vec{e}_r \times \vec{\tau})_i , \end{aligned} \quad (8)$$

with the SU(2) Pauli matrices $\vec{\tau} = (\tau_1, \tau_2, \tau_3)$. In the SO(3)-embedding $\vec{T} = (\lambda_7, -\lambda_5, \lambda_2)$, and the corresponding ansatz for the gauge field with vanishing time component is

$$\begin{aligned} A_0 &= 0 , \\ A_i &= \frac{2-K(r)}{2re}(\vec{e}_r \times \vec{\Lambda})_i + \frac{H(r)}{2re}[(\vec{e}_r \times \vec{\Lambda})_i, \vec{e}_r \cdot \vec{\Lambda}]_+ , \end{aligned} \quad (9)$$

where $[\ , \]_+$ denotes the anticommutator, and $\vec{\Lambda} = (\lambda_7, -\lambda_5, \lambda_2)$.

The SU(2)-embedding, eq. (8), leads to the well studied SU(2) Einstein-Yang-Mills equations [1, 7, 8, 9]. To obtain the SU(3) Einstein-Yang-Mills equations for the SO(3)-embedding, eq. (9), we also employ the tt and rr components of the Einstein equations, yielding for the metric functions

$$\mu' = N(K'^2 + H'^2) + \frac{1}{8x^2} \left((K^2 + H^2 - 4)^2 + 12K^2H^2 \right) , \quad (10)$$

$$A' = \frac{2}{x}(K'^2 + H'^2)A , \quad (11)$$

where we have introduced the dimensionless mass function

$$\mu = \frac{e}{\sqrt{4\pi G}}m = \frac{em_{\text{Pl}}}{\sqrt{4\pi}}m \quad (12)$$

and the dimensionless coordinate $x = (e/\sqrt{4\pi G})r$, and the prime indicates the derivative with respect to x . For the matter field functions we obtain the equations

$$(ANK')' = \frac{1}{4x^2}AK \left(K^2 + 7H^2 - 4 \right) , \quad (13)$$

$$(ANH')' = \frac{1}{4x^2}AH \left(H^2 + 7K^2 - 4 \right) . \quad (14)$$

With help of eq. (11) the metric function A can be eliminated from the matter field equations. Note, that the equations are symmetric with respect to an interchange of the functions $K(x)$ and $H(x)$, and to the transformations $K(x) \rightarrow -K(x)$, and $H(x) \rightarrow -H(x)$, yielding degenerate solutions.

Comparing the equations of the SO(3) embedding to those of the SU(2) embedding [1] shows that to each SU(2) solution there corresponds a scaled SO(3) solution. Defining $x = 2\tilde{x}$, and $\mu = 2\tilde{\mu}$ the functions $K(x) = 2w(\tilde{x})$, $H(x) = 0$ satisfy the SO(3) equations with coordinate x , when the function w satisfies the SU(2) equations with coordinate \tilde{x} . Thus these SO(3) solutions have precisely double the mass of their SU(2) counterparts.

3 Regular Solutions

Let us first consider the regular solutions of the SU(3) Einstein-Yang-Mills system. Requiring asymptotically flat solutions implies that the metric functions A and μ both approach a constant at infinity, and that the matter functions approach a vacuum configuration of the gauge field. We here adopt

$$A(\infty) = 1 , \quad (15)$$

thus fixing the time coordinate, and

$$K(\infty) = \pm 2 , \quad H(\infty) = 0 , \quad (16)$$

$$K(\infty) = 0 , \quad H(\infty) = \pm 2 . \quad (17)$$

At the origin regularity of the solutions requires

$$\mu(0) = 0 , \quad (18)$$

and the gauge field functions must satisfy

$$K(0) = \pm 2, \quad H(0) = 0, \quad (19)$$

$$K(0) = 0, \quad H(0) = \pm 2. \quad (20)$$

Because of the symmetries of the $SO(3)$ Einstein-Yang-Mills equations it is sufficient to study solutions with $K(0) = 2$ and $H(0) = 0$. The other boundary conditions lead to degenerate solutions.

In the following we present some numerical results for the regular solutions of the $SO(3)$ embedding. In Table 1 we show the mass $\tilde{\mu} = \mu/2$ of the lowest $SO(3)$ solutions. Their ADM mass is

$$m_{ADM} = \mu(\infty) \sqrt{4\pi} \frac{m_{Pl}}{e}. \quad (21)$$

We observe, that the two lowest solutions, missed in the previous analysis by Künzle [12], have a smaller mass than the lowest scaled $SU(2)$ solution.

To compare with the $SO(3)$ solutions found by Künzle [12] we note, that his functions u_1 and u_2 are related to the functions K and H as follows

$$u_1(x) = \frac{K(x) + H(x)}{2}, \quad (22)$$

$$u_2(x) = \frac{K(x) - H(x)}{2}, \quad (23)$$

with the boundary conditions at the origin $u_1(0) = u_2(0) = 1$, and at infinity $u_1(\infty) = \pm 1$ and $u_2(\infty) = \pm 1$.

Let us adopt the classification of the solutions with respect to their boundary conditions at infinity, the nodes (n_1, n_2) of the functions (u_1, u_2) [12], and the total number of nodes $n = n_1 + n_2$. We see in Table 1, that the lowest $SO(3)$ solution has the node structure $(0, 1)$, i. e. $n = 1$. In contrast, the lowest scaled $SU(2)$ solution, being the lowest $SO(3)$ solution found by Künzle [12], has the node structure $(1, 1)$, i. e. $n = 2$. Naturally, the mass of the $SO(3)$ solution with one node only is lower than the mass of the scaled $SU(2)$ solution with $n = 2$. But there is a second $SO(3)$ solution with a lower mass. This solution has the node structure $(0, 2)$, i. e. a total of two nodes like the lowest scaled $SU(2)$ solution. Evidently, the whole class of solutions with node structure $(0, n)$ has been missed before [12]. This class contains the lowest $SO(3)$ solution, and for a given total number of nodes, these new solutions appear to be lowest.

Table 1 further gives the coefficients β_1 and β_2 for the numerical integration with the shooting method [12]

$$u_1(\tilde{x}) = 1 + \beta_1 \tilde{x}^2 + \beta_2 \tilde{x}^3 + \dots, \quad (24)$$

$$u_2(\tilde{x}) = 1 + \beta_1 \tilde{x}^2 - \beta_2 \tilde{x}^3 + \dots. \quad (25)$$

In Figs. 1-4 we show the lowest SO(3) solution. It is obtained independently in the limit of vanishing coupling constant on the unstable upper branch of the Einstein-Skyrme system [13]. The excited solutions and further details will be given elsewhere [16].

The instability of the regular solutions follows from Theorem 1 of Ref. [15]. There the instability of the solutions of Künzle [12] was demonstrated. We find that the theorem applies also to the new class of solutions with node structure $(0, n)$, including the lowest mass solution (where $\alpha = 1$ [15] as well).

4 Black Hole Solutions

We now turn to the black hole solutions of the SU(3) Einstein-Yang-Mills system. Imposing again the condition of asymptotic flatness, the black hole solutions satisfy the same boundary conditions at infinity as the regular solutions. The existence of a regular event horizon at x_H requires

$$\mu(x_H) = \frac{x_H}{2} , \quad (26)$$

and $A(x_H) < \infty$, and the matter functions must satisfy at the horizon x_H

$$N'K' = \frac{1}{4x^2}K\left(K^2 + 7H^2 - 4\right) , \quad (27)$$

$$N'H' = \frac{1}{4x^2}H\left(H^2 + 7K^2 - 4\right) . \quad (28)$$

SO(3) black hole solutions have not been found previously [12]. In Fig. 5 we exhibit the masses of the lowest SO(3) black holes in terms of the mass fractions outside the horizon, μ_{out} , defined via

$$m_{\text{ADM}} = \left(\frac{x_H}{2} + \mu_{\text{out}}\right)\frac{\sqrt{4\pi}m_{\text{Pl}}}{e} = \mu(\infty)\frac{\sqrt{4\pi}m_{\text{Pl}}}{e} , \quad (29)$$

as a function of the horizon x_H . For $x_H \rightarrow 0$ the black hole solutions approach the regular solutions. With increasing horizon x_H these black hole solutions keep their identity in terms of the boundary conditions and the node structure. Only the second solution with node structure $(1, 1)$ (#4 of Table 1) disappears. This solution has the same boundary conditions and node structure as the lowest scaled SU(2) solution (#3 of Table 1), but a slightly higher mass. It in fact merges into the scaled SU(2) solution at a horizon of $x_H = 1.7146$, leaving a unique black hole solution with node structure $(1, 1)$. (The same feature holds for the two solutions with node structure $(2, 2)$ of Ref. [12]. The solution with higher mass merges into the solution with lower mass, again a scaled SU(2) solution, at a horizon of $x_H = 1.3745$.) Note, that the order of the solutions

changes from the order of the regular solutions as the horizon increases. For instance, beyond $x_H = 0.703$ solution #5 has a lower mass than solution #3.

In Table 2 we present some properties of the black hole solutions with a horizon $x_H = 1$, emerging from the first five regular solutions of Table 1, using again the notation of Ref. [12]. The table contains the values of the functions u_1 and u_2 at the horizon, needed for a numerical shooting procedure.

The families of $SO(3)$ black hole solutions change continuously as a function of the horizon x_H . As examples we show the radial functions for the lowest $SO(3)$ black hole solutions for the horizons $x_H = 1, 2, 3, 4$ in Figs. (1)-(4). Further details of these solutions and the excited $SO(3)$ Einstein-Yang-Mills black holes will be given elsewhere [16].

The instability of the black hole solutions follows from Theorem 2 of Ref. [15]. We find that the theorem applies to all black hole solutions constructed (where $\alpha = 1$ [15] as well).

5 Conclusion

The $SU(3)$ Einstein-Yang-Mills system possesses a sequence of regular spherically symmetric solutions based on the $SO(3)$ embedding, besides the well-studied sequence based on the $SU(2)$ embedding [1]. The $SO(3)$ solutions can be labelled according to their node structure with two integers (n_1, n_2) and the total number of nodes n . The lowest solution has node structure $(0, 1)$ and $n = 1$. The first excited solution has node structure $(0, 2)$, while the second excited solution, the lowest scaled $SU(2)$ solution, has node structure $(1, 1)$. The third excited solution [12] has the same node structure as the lowest scaled $SU(2)$ solution, being only slightly higher in mass. The next solution then has $n = 3$, again with node structure $(0, n)$, suggesting that this class of solutions has the lowest mass for a given total number of nodes.

The regular $SU(2)$ solutions are known to be unstable [2, 3], the solution with n nodes has $2n$ unstable modes [4, 5]. The $SO(3)$ solutions are unstable as well, since Theorem 1 of Ref.[15] applies. It is an interesting open problem to study the number of unstable modes and find a relation to the number of nodes.

The lowest $SU(2)$ solution has been interpreted in analogy to the electroweak sphaleron [6] as the top of a barrier between vacua [3]. Furthermore, like the electroweak sphaleron [17, 18], the gravitating sphaleron also possesses a fermion zero mode [19] and gives rise to level-crossing [19, 20]. It appears to be interesting to study fermions also in the background of the lowest $SO(3)$ solution.

Corresponding to each regular $SO(3)$ solution there exist black hole solutions. These solutions keep their identity in terms of the node structure, for arbitrary horizon. If there are several solutions with the same structure of nodes, solutions may disappear

by merging with the lowest solution of a given node structure, as is for instance the case for the lowest scaled $SU(2)$ solution and its excitation with node structure (1,1).

The $SU(2)$ black holes are known to be unstable [10, 11, 5]. The $SO(3)$ black hole solutions are unstable as well, since Theorem 2 of Ref.[15] applies. It is an interesting open problem, especially with respect to the bifurcations, to study the number of unstable modes of the $SO(3)$ black holes.

Since the $SU(3)$ Einstein-Yang-Mills system also contains Schwarzschild black holes, there are then many static, neutral black hole solutions (including the $SU(2)$ black holes) for a given mass, enlarging the counterexample to the “no-hair conjecture”. But only the Schwarzschild solution is stable. The coloured black holes are all unstable.

Charged $SU(3)$ black hole solutions have been considered previously [21], and $SU(2) \times U(1)$ solutions have been constructed [21]. Here a natural extension is to consider charged $SO(3)$ black hole solutions.

Acknowledgement

We gratefully acknowledge discussions with M. Volkov.

References

- [1] R. Bartnik, and J. McKinnon, Particlelike solutions of the Einstein-Yang-Mills equations, *Phys. Rev. Lett.* 61 (1988) 141.
- [2] N. Straumann, and Z. H. Zhou, Instability of the Bartnik-McKinnon solutions of the Einstein-Yang-Mills equations, *Phys. Lett.* B237 (1990) 353.
- [3] D. V. Gal'tsov, and M. S. Volkov, Sphalerons in Einstein-Yang-Mills theory, *Phys. Lett.* B273 (1991) 255.
- [4] G. Lavrelashvili, and D. Maison, A remark on the instability of the Bartnik-McKinnon solutions, *Phys. Lett.* B343 (1995) 214.
- [5] M. S. Volkov, O. Brodbeck, G. Lavrelashvili, and N. Straumann, The number of sphaleron instabilities of the Bartnik-McKinnon solitons and nonabelian black holes, preprint ZU-TH-3-95, hep-th/9502045.
- [6] F. R. Klinkhamer, and N. S. Manton, A saddle-point solution in the Weinberg-Salam theory, *Phys. Rev.* D30 (1984) 2212.
- [7] M. S. Volkov, and D. V. Galt'sov, Black holes in Einstein-Yang-Mills theory, *Sov. J. Nucl. Phys.* 51 (1990) 747.
- [8] P. Bizon, Colored black holes, *Phys. Rev. Lett.* 64 (1990) 2844.

- [9] H. P. Künzle and A. K. M. Masoud-ul-Alam, Spherically symmetric static $SU(2)$ Einstein-Yang-Mills fields, *J. Math. Phys.* 31 (1990) 928
- [10] N. Straumann, and Z. H. Zhou, Instability of colored black hole solutions, *Phys. Lett.* B243 (1990) 33.
- [11] M. S. Volkov, and D. V. Gal'tsov, Odd-parity negative modes of Einstein-Yang-Mills black holes and sphalerons, *Phys. Lett.* B341 (1995) 279.
- [12] H. P. Künzle, Analysis of the static spherically symmetric $SU(n)$ -Einstein-Yang-Mills equations, *Comm. Math. Phys.* 162 (1994) 371.
- [13] B. Kleihaus, J. Kunz, and A. Sood, $SU(3)$ Einstein-Skyrme solitons and black holes, Utrecht preprint THU-95/6, hep-th/9503087.
- [14] P. Bizon, and T. Chmaj, Gravitating skyrmions, *Phys. Lett.* B297 (1992) 55.
- [15] O. Brodbeck, and N. Straumann, Instability proof for Einstein-Yang-Mills solitons and black holes with arbitrary gauge groups, ZU-TH-38-94, gr-qc/9411058.
- [16] B. Kleihaus, J. Kunz, and A. Sood, in preparation.
- [17] J. Boguta, and J. Kunz, Hadroids and sphalerons, *Phys. Lett.* B154 (1985) 407.
- [18] J. Kunz, and Y. Brihaye, Fermions in the background of the sphaleron barrier, *Phys. Lett.* B304 (1993) 141.
- [19] G. W. Gibbons, and A. R. Steif, Anomalous fermion production in gravitational collapse, *Phys. Lett.* B314 (1993) 13.
- [20] M. S. Volkov, Einstein-Yang-Mills sphalerons and level crossing, *Phys. Lett.* B334 (1994) 40.
- [21] D. V. Gal'tsov, and M. S. Volkov, Charged non-abelian $SU(3)$ Einstein-Yang-Mills black holes, *Phys. Lett.* B274 (1992) 173.

	$\tilde{\mu}(\infty)$	nodes		β_1	β_2	$u_1(\infty)$	$u_2(\infty)$	
		u_1	u_2					
1	0.65389	0	1	-.41172	0.25397	1	-1	
2	0.81130	0	2	-.60281	0.39068	1	1	
3	0.82865	1	1	-.45372	0	-1	-1	scaled SU(2)
4	0.84769	1	1	-.53766	0.26077	-1	-1	Künzle
5	0.85237	0	3	-.67272	0.43953	1	-1	
6	0.93774	1	2	-.63437	0.33228	-1	1	Künzle

Table 1: Properties of the lowest regular SO(3) solutions are given in the notation of Ref. [12]. The ADM mass is obtained from the second column via Eq. (21) with $\mu(\infty) = 2\tilde{\mu}(\infty)$, the third and forth column give the number of nodes of the functions u_1 and u_2 defined in Eqs. (22)-(23), the fifth and sixth column provide the expansion coefficients of these functions as defined in Eqs. (24)-(25), and the seventh and eighth column give the values of the functions u_1 and u_2 at infinity.

	$\tilde{\mu}(\infty)$	nodes		$u_1(\tilde{x}_H)$	$u_2(\tilde{x}_H)$	$u_1(\infty)$	$u_2(\infty)$	
		u_1	u_2					
1	0.70796	0	1	0.92330	0.90406	1	-1	
2	0.82592	0	2	0.88653	0.84925	1	1	
3	0.86855	1	1	0.89723	0.89723	-1	-1	scaled SU(2)
4	0.87410	1	1	0.89501	0.87557	-1	-1	
5	0.85608	0	3	0.87481	0.83035	1	-1	

Table 2: Properties of the lowest SO(3) black hole solutions are given for the horizon $x_H = 1 = 2\tilde{x}_H$ following the classification of Table 1. The ADM mass is obtained from the second column via Eq. (21) with $\mu(\infty) = 2\tilde{\mu}(\infty)$, the third and forth column give the number of nodes of the functions u_1 and u_2 defined in Eqs. (22)-(23), the fifth and sixth column provide the value of these functions at the horizon, and the seventh and eighth column give the values of the functions u_1 and u_2 at infinity.

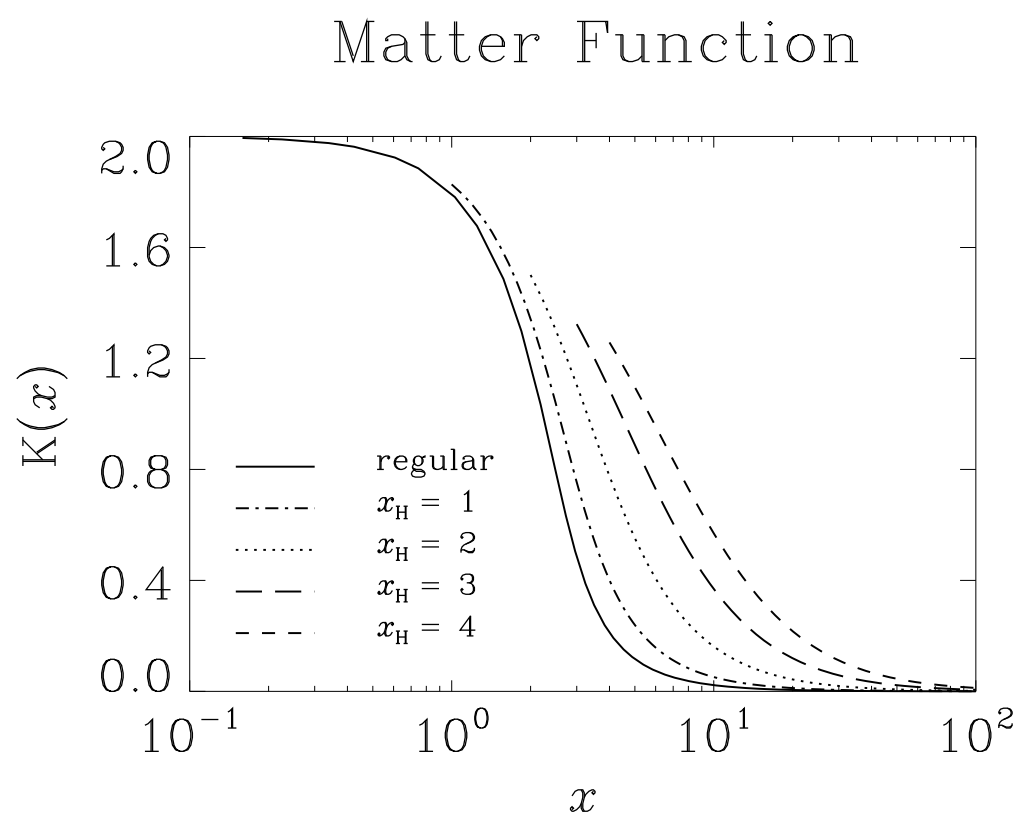


Figure 1: The function $K(x)$ is shown for the regular solution and for the black hole solutions with horizons $x_H = 1, 2, 3$ and 4 as a function of x .

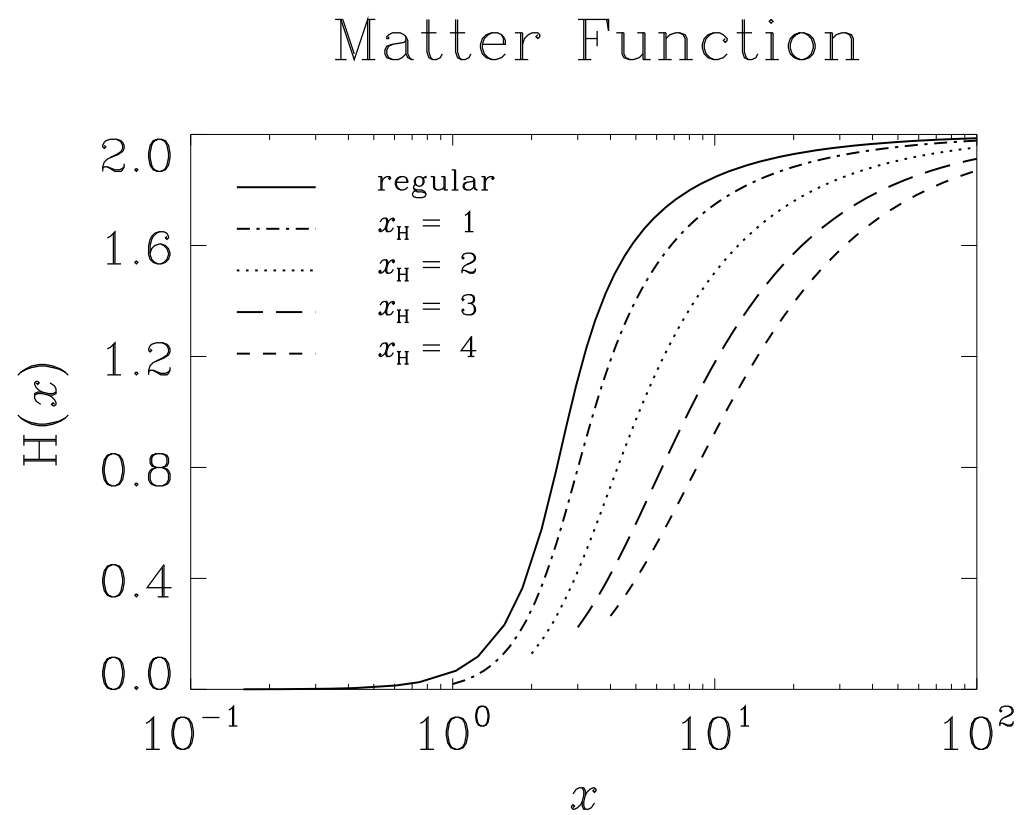


Figure 2: The function $H(x)$ is shown for the regular solution and for the black hole solutions with horizons $x_H = 1, 2, 3$ and 4 as a function of x .

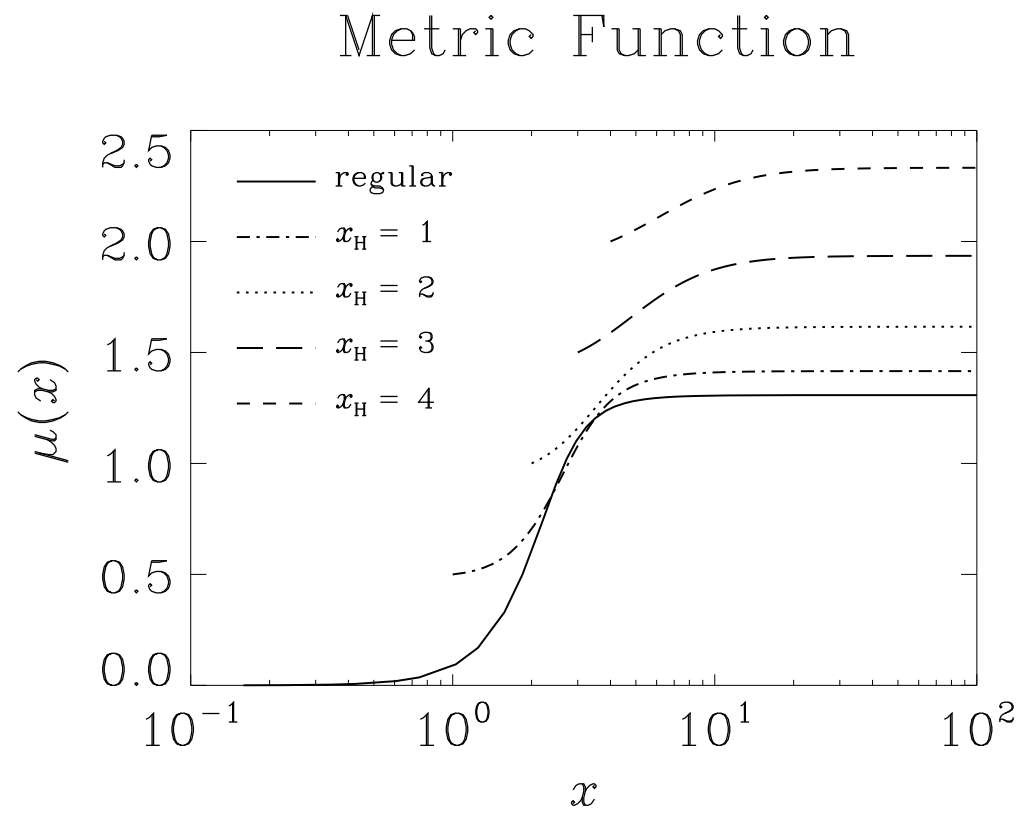


Figure 3: The function $\mu(x)$ is shown for the regular solution and for the black hole solutions with horizons $x_H = 1, 2, 3$ and 4 as a function of x .

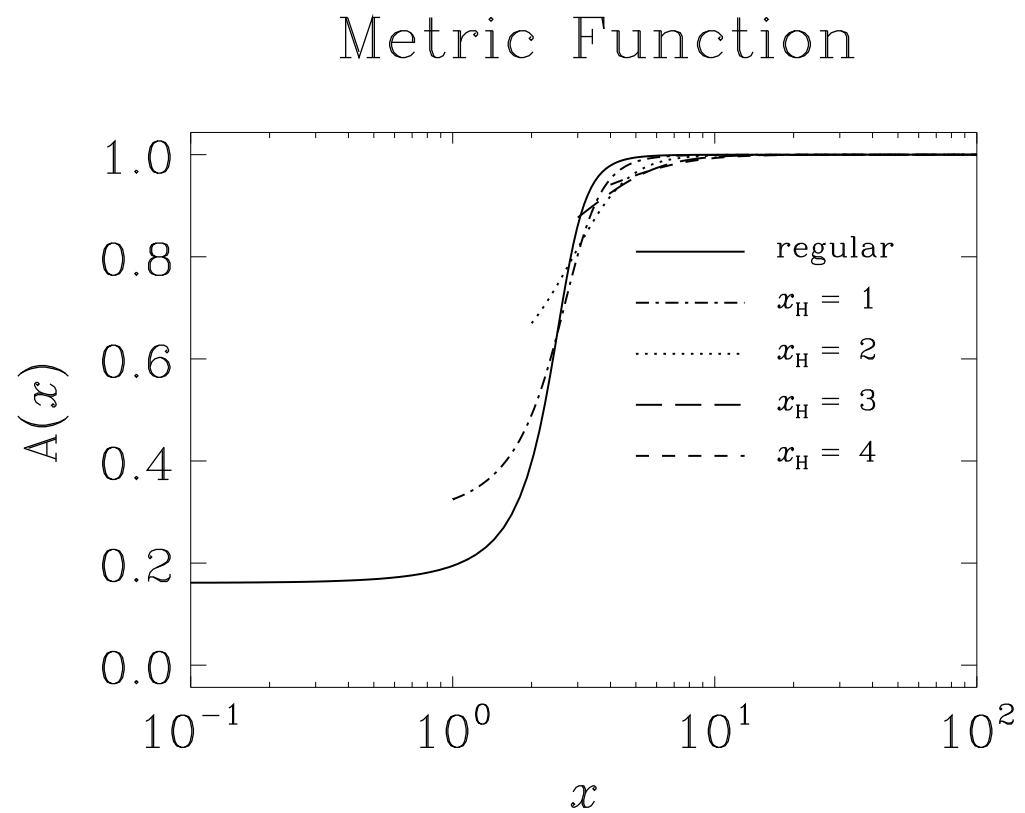


Figure 4: The function $A(x)$ is shown for the regular solution and for the black hole solutions with horizons $x_H = 1, 2, 3$ and 4 as a function of x .

Mass vs. Event Horizon

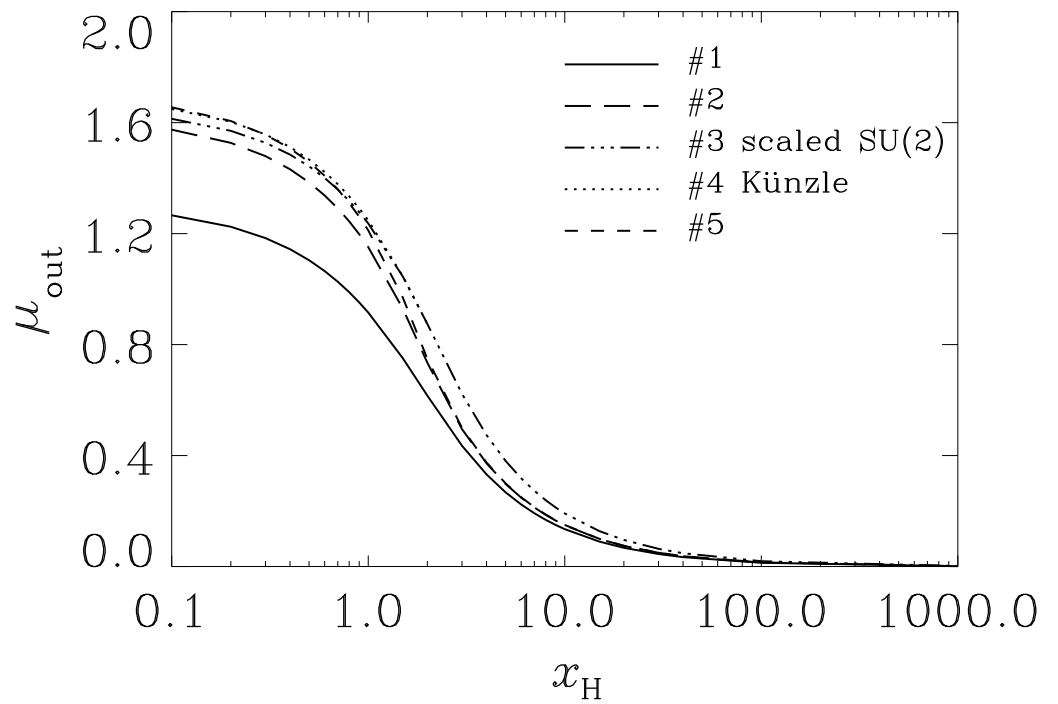


Figure 5: The mass fraction outside the horizon, μ_{out} , of the SO(3) black hole solutions of Table 2 is shown as a function of the horizon x_{H} . When the mass fraction within the horizon, $x_{\text{H}}/2$, is added, the ADM mass is obtained.